Supplementary Information for

High geomagnetic field intensity recorded by anorthosite xenoliths requires a vigorous late Mesoproterozoic geodynamo

Yiming Zhang, Nicholas L. Swanson-Hysell, Margaret S. Avery, Roger R. Fu

Yiming Zhang
E-mail: yimingzhang@berkeley.edu

This PDF file includes:

Figs. S1 to S4 (not allowed for Brief Reports)
Tables S1 to S2 (not allowed for Brief Reports)
SI References

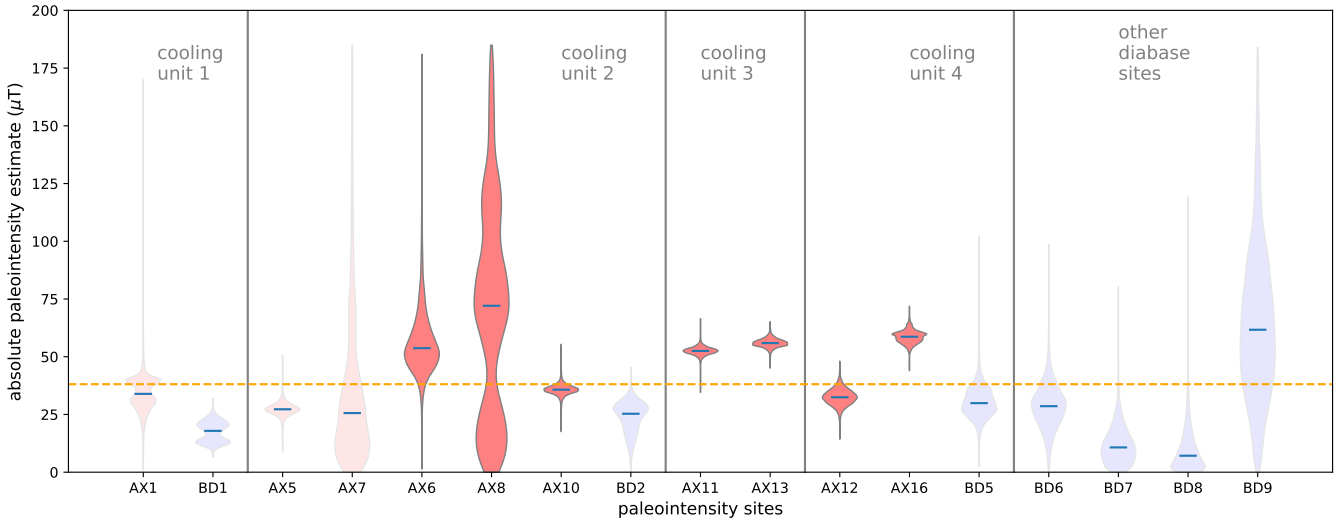

Fig. S1. Violin plots of site-level posterior paleointensity distributions estimated using the bias corrected estimation of paleointensity (BiCEP) method developed by ref. **??**. Assuming that paleointensity estimates from specimens that come from a same cooling unit are distributed around a true paleointensity value with the various deflections being expressed as the curvature parameter of the NRM/TRM plot (1, 2), the method uses all paleointensity measurement-level data without applying selection criteria. For comparison of results from this independent method with those based on our selection (as show in Fig. 4 in manuscript), we highlight the anorthosite sites that pass our paleointensity selection and make other anorthosite and diabase transparent. The results from the BiCEP method address the uncertainties associated with anorthosite AX6 and AX8. This is associated with the relatively variable specimen behaviors within these two sites. But for sites AX10, AX11, AX13, AX12, and AX16, the posterior probability distributions have very narrow bounds, consistent with the interpretation that these anorthosites are faithful paleointensity recorders that have high-quality paleointensity behaviors.

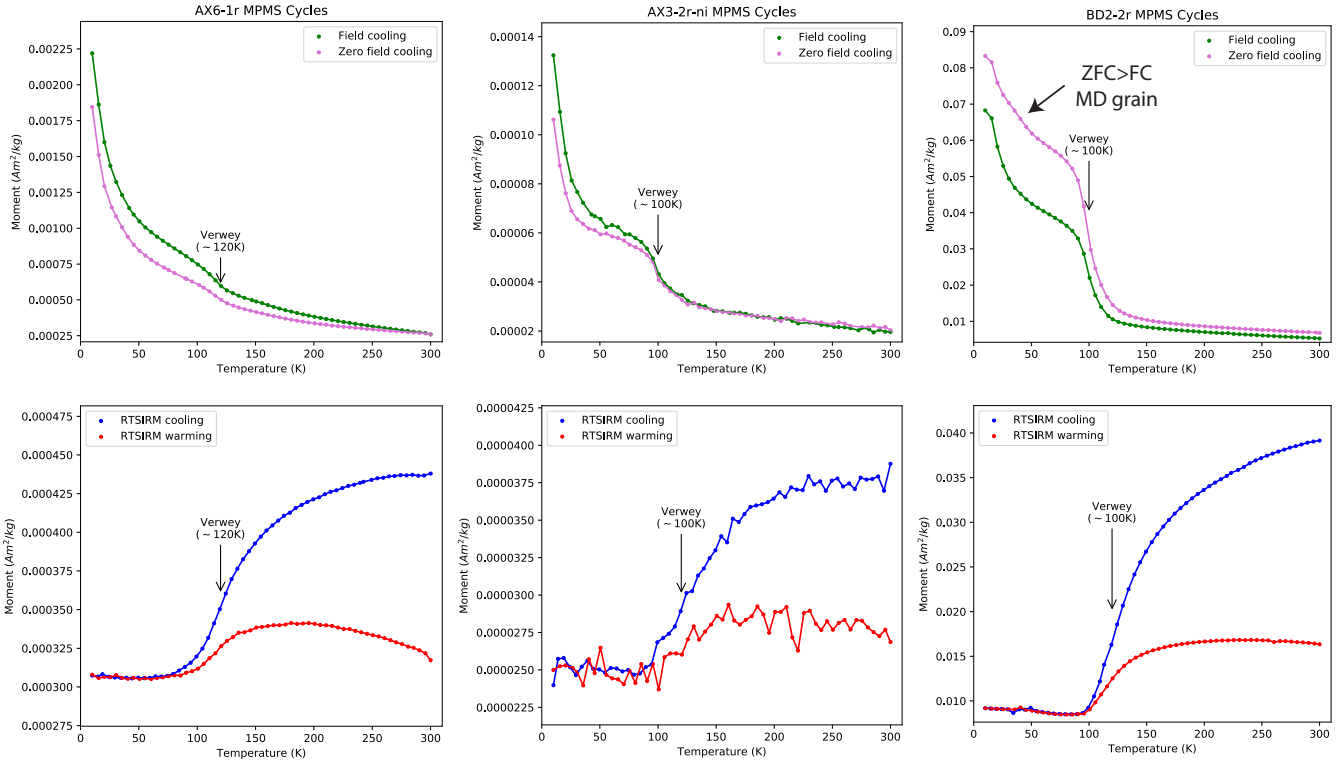

Fig. S2. Low-temperature magnetic property measurement system (MPMS) experiment results. In the field-cooled (FC) experiments, the magnetization was measured upon warming following the specimen having cooled in an applied field of 2.5 T from 300 to 10 K. In the zero-field-cooled (ZFC) experiment, a low-temperature saturation isothermal remanence (LTSIRM) of 2.5 T was applied at 10 K after the specimen cooled in a (near-)zero field. In the room-temperature saturation isothermal remanence (RTSIRM) experiment, the sample was pulsed with a 2.5 T field at room temperature (∼300 K) and then cooled to 10 K and warmed back to room temperature in a (near-) zero field. Specimen AX6-1r is from anorthosite AX6 which passed our paleointensity selection. It has a well-defined Verwey transition ∼120 K (3). Specimens AX3-2r-ni and BD2-2r show Verwey transition but the transition temperatures are suppressed below ∼120 K. Specimen BD2-2r has a consistently higher moment during the zero-field-cooled step than during the field-cooled step. This is consistent with the interpretation that multidomian magnetic carriers exist in significant quantity in this specimen.

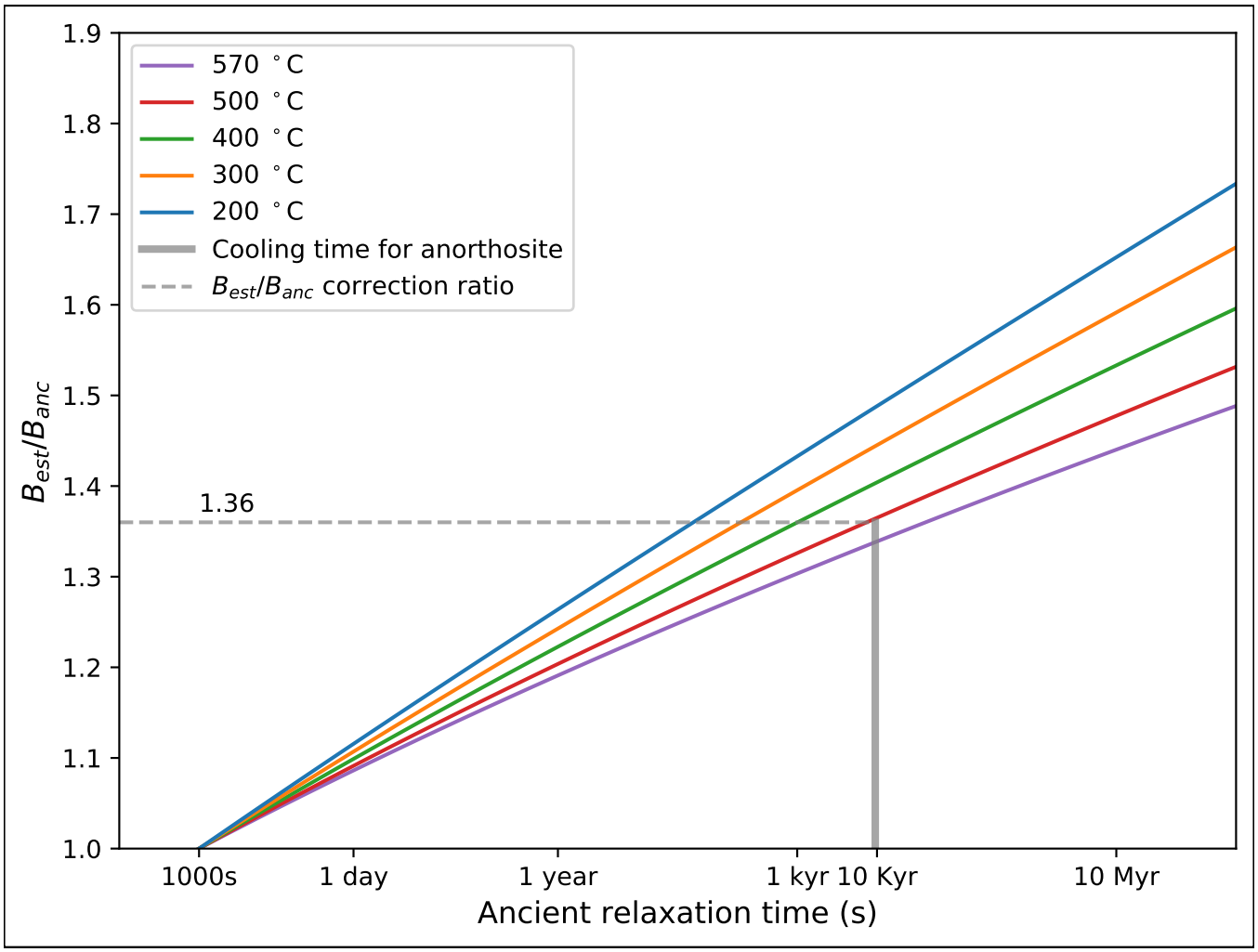

Fig. S3. Graph of predicted paleointensity overestimate due to slow cooling of the intrusive Beaver River diabase and anorthosite xenoliths relative to the cooling rate in laboratory following the model of Halgedahl1980a. Because the majority of the anorthosites have unblocking temperatures between 500℃ and 580℃, we estimate that the slow cooling during natural remanence acquisition could have resulted in a 36% overestimate. Thus, a correction factor of 0.74 is applied at specimen level for the paleointensity summary plot.

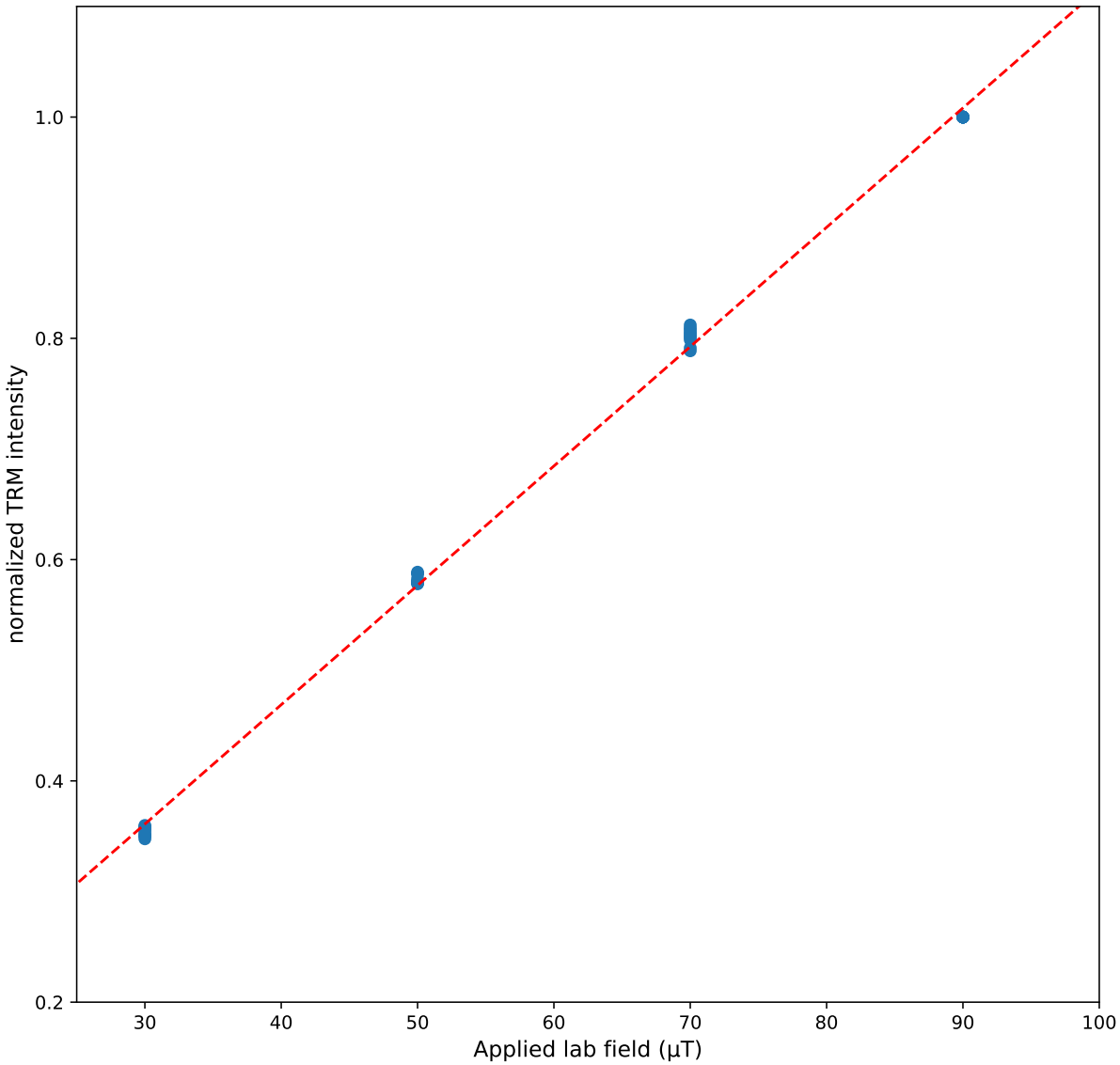

Fig. S4. Plot of linear thermal remanent magnetization acquisition experiment results. After IZZI-type Thellier paleointensity experiments, full TRMs were imparted on the same specimens in known lab fields of 30, 50, 70, and 90 μT. The red dashed line shows a linear fit through the data points. The results show that the anorthosite xenoliths do not acquire saturation remanence or display non-linear remanence acquisition under fields relevant to this study. Therefore, non-linear acquisition correction is not needed for our paleointensity results.

Table S1. **Summary paleointensity results for specimens that passed our selection. Paleointensity results for specimens that passed quality criteria. B_{anc} is the calculated ancient field intensity over the chosen temperature interval in μT. T_{min} and T_{max} indicate the temperature interval over which the best fit for paleointensity was defined. N is the number of steps used within the selected interval for paleointensity determination. FRAC is the fraction of remanence. NpTRM shows the number of pTRM checks within the selected interval for paleointensity determination. β is the scatter parameter. GAP-MAX is the maximum magnetization gap between two adjacent steps. MAD is the maximum angle of deviation. DANG is the deviation angle. SCAT is the scatter parameter. Paleolatitude is calculated from the inclination values reported in (4). γ is the gamma statistic that measures the angle between the last pTRM step used for paleointensity determination and the applied field direction. V(A)DM is the virtual (axial) dipole moment reported in 10^{21} Am^2 (ZAm^2).**

Site	Specimen	B_{anc}	T_{min}	T_{max}	N	FRAC	NpTRM	β	GAP-MAX	MAD (°)	DANG (°)	SCAT	Paleolatitude	γ	VADM (ZAm^2)
AX6	AX6-2a	18.25	400	585	18	0.7	10.0	0.04	0.12	3.44	3.43	PASS	15.61	2.7	31.69
AX6	AX6-3a	25.39	400	585	18	0.76	10.0	0.04	0.1	4.28	2.88	PASS	15.61	3.2	44.08
AX6	AX6-1a	49.13	425	585	17	0.71	10.0	0.03	0.14	4.45	0.96	PASS	15.61	2.0	85.3
AX8	AX8-3a	41.3	400	580	17	0.75	9.0	0.03	0.14	4.38	2.22	PASS	17.16	11.2	70.45
AX8	AX8-1a	66.18	450	570	13	0.68	8.0	0.06	0.18	4.54	2.37	PASS	17.16	7.0	112.88
AX10	AX10-1a	45.84	425	585	17	0.78	10.0	0.06	0.24	5.6	2.62	PASS	14.41	4.7	80.64
AX10	AX10-3a	48.01	425	585	17	0.69	10.0	0.04	0.24	4.02	1.56	PASS	14.41	5.8	84.45
AX10	AX10-2a	48.23	425	585	17	0.67	10.0	0.05	0.19	5.3	1.93	PASS	14.41	7.8	84.84
AX11	AX11-1a	73.29	425	560	10	0.67	6.0	0.08	0.21	5.28	2.54	PASS	12.27	5.9	131.75
AX11	AX11-2a	73.29	400	560	11	0.65	6.0	0.07	0.21	3.94	1.51	PASS	12.27	9.9	131.75
AX11	AX11-4a	73.31	500	570	11	0.66	8.0	0.09	0.2	1.53	3.27	PASS	12.27	5.6	131.78
AX11	AX11-6a	73.32	200	562	14	0.69	7.0	0.07	0.17	4.0	1.33	PASS	12.27	3.0	131.8
AX11	AX11-9a	73.34	100	562	15	0.67	7.0	0.06	0.17	5.34	1.13	PASS	12.27	11.9	131.84
AX11	AX11-3a	73.41	400	560	11	0.66	6.0	0.08	0.21	3.95	2.11	PASS	12.27	8.2	131.96
AX11	AX11-5a	73.44	400	566	14	0.73	8.0	0.05	0.18	2.93	0.85	PASS	12.27	1.9	132.02
AX12	AX12-14a	30.34	475	585	16	0.75	10.0	0.06	0.17	1.74	0.55	PASS	24.54	0.9	47.18
AX12	AX12-1a	33.89	0	580	21	0.97	9.0	0.03	0.17	5.47	4.73	PASS	24.54	10.0	52.7
AX12	AX12-6a	37.18	425	564	12	0.69	7.0	0.08	0.22	3.64	2.05	PASS	24.54	5.0	57.81
AX12	AX12-8a	38.34	475	565	12	0.75	8.0	0.06	0.25	1.46	2.29	PASS	24.54	1.6	59.62
AX12	AX12-4a	41.89	500	585	14	0.66	10.0	0.05	0.24	3.85	3.19	PASS	24.54	11.4	65.14
AX12	AX12-2a	46.94	425	570	14	0.7	8.0	0.05	0.24	3.39	2.38	PASS	24.54	7.0	72.99
AX13	AX13-3a	71.68	100	550	12	0.71	5.0	0.08	0.22	5.92	1.88	PASS	11.25	3.4	130.08
AX13	AX13-4a	75.42	200	555	12	0.7	6.0	0.03	0.17	7.28	0.41	PASS	11.25	3.7	136.87
AX13	AX13-6a	76.8	200	555	12	0.7	6.0	0.06	0.22	3.82	1.53	PASS	11.25	4.5	139.37
AX13	AX13-2a	76.96	300	555	11	0.69	6.0	0.05	0.2	7.87	2.73	PASS	11.25	4.1	139.66
AX13	AX13-9a	77.48	0	564	17	0.94	7.0	0.03	0.16	5.96	1.07	PASS	11.25	2.6	140.61
AX13	AX13-8a	84.83	450	570	13	0.81	8.0	0.02	0.24	3.69	1.82	PASS	11.25	5.1	153.94
AX16	AX16-13a	41.68	400	570	15	0.72	8.0	0.07	0.2	3.47	1.85	PASS	22.11	1.1	66.88
AX16	AX16-16a	42.2	400	570	15	0.77	8.0	0.06	0.15	3.9	1.81	PASS	22.11	2.0	67.72
AX16	AX16-14a	43.57	400	570	15	0.71	8.0	0.06	0.13	3.25	1.79	PASS	22.11	6.0	69.91
AX16	AX16-11a	44.17	450	570	14	0.7	8.0	0.06	0.15	2.86	2.07	PASS	22.11	4.6	70.88
AX16	AX16-5a	45.75	400	560	11	0.69	6.0	0.09	0.22	7.98	4.32	PASS	22.11	4.0	73.41
AX16	AX16-4a	45.96	425	570	14	0.75	8.0	0.05	0.21	5.01	1.18	PASS	22.11	4.2	73.75
AX16	AX16-2a	45.98	400	564	13	0.68	7.0	0.06	0.21	4.37	1.57	PASS	22.11	4.9	73.78
AX16	AX16-1a	46.25	200	562	14	0.85	7.0	0.07	0.23	6.04	2.87	PASS	22.11	4.5	74.22
AX16	AX16-9a	48.9	475	585	16	0.66	10.0	0.04	0.16	2.92	1.4	PASS	22.11	4.3	78.47
AX16	AX16-10a	54.02	500	585	15	0.66	10.0	0.04	0.18	2.78	1.15	PASS	22.11	5.5	86.68

Table S2. **Summary statistics for the Q_{PI} quality criteria of (5).**

Site	N	Age (Ma)	Method	AGE	STAT	TRM	ALT	MD	ACN	TECH	LITH	QPI
AX6	3	1091.8	T+	1	0	1	1	1	1	0	0	5
AX8	2	1091.8	T+	1	0	1	1	1	1	0	0	5
AX10	3	1091.8	T+	1	0	1	1	1	1	0	0	5
AX11	7	1091.8	T+	1	1	1	1	1	1	0	0	6
AX12	6	1091.8	T+	1	1	1	1	1	1	0	0	6
AX13	7	1091.8	T+	1	1	1	1	1	1	0	0	6
AX16	11	1091.8	T+	1	1	1	1	1	1	0	0	6

References

1. Y Arai, Secular variation in intensity of the past geomagnetic field. *M.Sc. thesis, Univ. Tokyo, Tokyo, Jpn.* (1963).
2. GA Paterson, A simple test for the presence of multidomain behavior during paleointensity experiments. *J. Geophys. Res.* **116** (2011).
3. EJW Verwey, Electronic Conduction of Magnetite (Fe3O4) and its Transition Point at Low Temperatures. *Nature* **144**, 327–328 (1939).
4. Y Zhang, NL Swanson-Hysell, MD Schmitz, JD Miller, MS Avery, Synchronous emplacement of the anorthosite xenolith-bearing Beaver River diabase and one of the largest lava flows on Earth. *Geochem. Geophys. Geosystems* (2021).
5. AJ Biggin, GA Paterson, A new set of qualitative reliability criteria to aid inferences on palaeomagnetic dipole moment variations through geological time. *Front. Earth Sci.* **2** (2014).